LM-02K102
October 10, 2002

Recombination Parameters for Antimonide-Based Semiconductors using RF Photoreflection Techniques

R.J. Kumar, J.M. Borrego, P.S. Dutta, R.J. Gutmann, C.A. Wang,
R.U. Martinelli, G. Nichols

02K102

Recombination Parameters for Antimonide-Based Semiconductors using RF Photoreflection Techniques

R. J. Kumar, J. M. Borrego, P. S. Dutta and R. J. Gutmann
Center for Integrated Electronics
Department of Electrical, Computer and Systems Engineering
Rensselaer Polytechnic Institute, Troy, NY 12180

C. A. Wang
Lincoln Laboratory
Lexington, MA 02420

R. U. Martinelli
Sarnoff Corporation
Princeton, NJ 08543

G. Nichols
Lockheed Martin
Schenectady, NY 12301

RF photoreflection measurements and PC-1D simulations have been used to evaluate bulk and surface recombination parameters in antimonide-based materials. PC-1D is used to simulate the photoconductivity response of antimonide-based substrates and doubly-capped epitaxial layers and also to determine how to extract the recombination parameters using experimental results. Excellent agreement has been obtained with a first-order model and test structure simulation when Shockley-Reed-Hall (SRH) recombination is the bulk recombination process. When radiative, Auger and surface recombination are included, the simulation results show good agreement with the model. RF photoreflection measurements and simulations using PC-1D are compatible with a radiative recombination coefficient (B) of approximately 5 x 10^{-11} cm^3/s, Auger coefficient (C) ~ 1.0 x 10^{-28} cm^6/s and surface recombination velocity (SRV) ~ 600 cm/s for 0.50 – 0.55 eV doubly-capped InGaAsSb material with GaSb capping layers using the experimentally determined active layer doping of 2 x 10^{17} cm^{-3}. Photon recycling, neglected in the analysis and simulations presented, will affect the extracted recombination parameters to some extent.

I. Introduction

Antimonide-based materials are promising candidates for thermophotovoltaic (TPV) cells, infrared lasers and high-speed photodetectors [1]. These minority carrier devices depend heavily on the various recombination processes to return an excited system to its equilibrium state. Therefore, evaluation of the minority-carrier lifetime and determination of the dominant recombination mechanism are important for these device applications.

Recent work has shown that radiative and / or Auger recombination (and not Shockley-Reed-Hall (SRH) recombination) is the dominant bulk recombination mechanism in these materials [2, 3]. Theoretical calculations and experiments give a radiative recombination coefficient value of approximately 5 x 10^{-11} cm^3/s for low bandgap antimonide materials. However, significant variations have been reported in the literature for the Auger coefficients (10^{-26} to 10^{-29} cm^6/s), as summarized by Charache et al. [4]. Theoretical calculations have also been done to evaluate the carrier lifetimes and the performance limits of these materials [5, 6]. The focus of this work is to obtain

improved values for the recombination parameters in these materials, particularly the Auger coefficients, using RF photoreflectance measurements and PC-1D simulations.

A radio-frequency (RF) photoreflectance technique, which senses changes in sample conductivity as carriers recombine following excitation by a laser pulse, is used for the measurements. Earlier work by Ahrenkiel et al. [7] and Saroop et al. [8] successfully applied this technique to characterize antimonide-based substrates and epitaxial layers using double heterostructure confinement. This work has shown that double-heterostructure capping for quaternary layers results in a surface recombination velocity (SRV) of 1300 cm/s for the InGaAsSb/AlGaAsSb interface and 1900 cm/s for the InGaAsSb/GaSb interface [8].

Doubly capped structures are important to limit the front and back surface recombination velocities to the order of ~ 10^3 cm/s, thereby allowing the photoconductivity decay transient to be sensitive to bulk recombination processes. In particular, the photoconductivity transient depends on the bulk lifetime and the thickness of the active layer, as well as the SRV if sufficiently high. In the case of thick (~ 500 μm) unpassivated substrates, the front surface SRV often controls the photoconductivity transient.

Analysis and/or simulation techniques are required to isolate bulk and surface effects with such samples. While previous work has focused on closed form analysis to indicate trends [8], this work uses a simulation tool (PC-1D) to model the sheet conductance transient response to above-bandgap optical excitation. Thus basic recombination parameters can be used in the model to isolate the effect of different mechanisms as a function of processing and characterization parameters.

II. Experimental Techniques

The RF Photoreflection system senses changes in the sample conductivity as carriers recombine following excitation by a laser pulse. A Laser Photonics YQL-102 Q-switched Nd:YAG laser operates at 1.06 μm with a nominal pulse width and decay time of 13.5 ns and 5 ns respectively. A schematic of the measurement system is shown in Figure 1 [8].

The continuous-wave RF carrier signal, obtained from a variable frequency oscillator set at 410 MHz, is fed to a tuned inductor-capacitor circuit forming the RF probe. The capacitor is adjusted so that the probe is critically coupled in the absence of a sample. When the coil is brought in proximity to any conducting sample, a transformer is formed with the coil as the primary and the induced eddy currents as a one-turn secondary. The sheet resistance of the sample is then transformed into an effective load resistance in the primary. Without photoexcitation, a fraction of the RF signal is reflected from the effective load resistance. The amplitude and phase of the reflected signal are detected by the balanced mixer and converted to a dc voltage, which is then digitized.

When the sample is illuminated by the laser, excess carriers generated cause an increase in conductivity. The modulated reflected signal is demodulated by the mixer, providing a transient signal whose amplitude is proportional to the change in sample conductivity, assuming that the impedance change is small compared to the measurement system impedance. More than one exponential decay time is usually observed, related to the optically-induced carrier injection level.

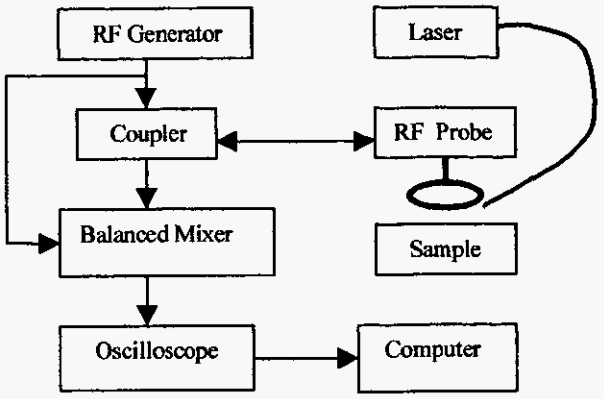

Figure 1. Schematic of RF Photoreflection system

The typical RF photoreflectance response for a GaSb substrate at a laser wavelength of 1064 nm and pulse energy 1.5 mJ/cm^2 is shown in Figure 2. The measured pulse height, initial decay time and long-decay times are indicated in the figure. Measurements at lower injection levels are carried out by placing optical filters in the path of the beam, thereby allowing measurements at intensities 15% and 5% of the original value.

The test structures used in this work include bulk GaSb substrates (n or p-doped and typically 500 μm thick) and quaternary (InGaAsSb) layers with double-heterostructure capping (carrier-confinement) layers, grown on GaSb substrates. The doubly capped structures consist of samples with GaSb capping layers (Figure 3). All layers are lattice matched to the InGaAsSb active layer and are grown by organometallic vapor phase epitaxy (OMVPE). The minority carriers are confined to the active region by

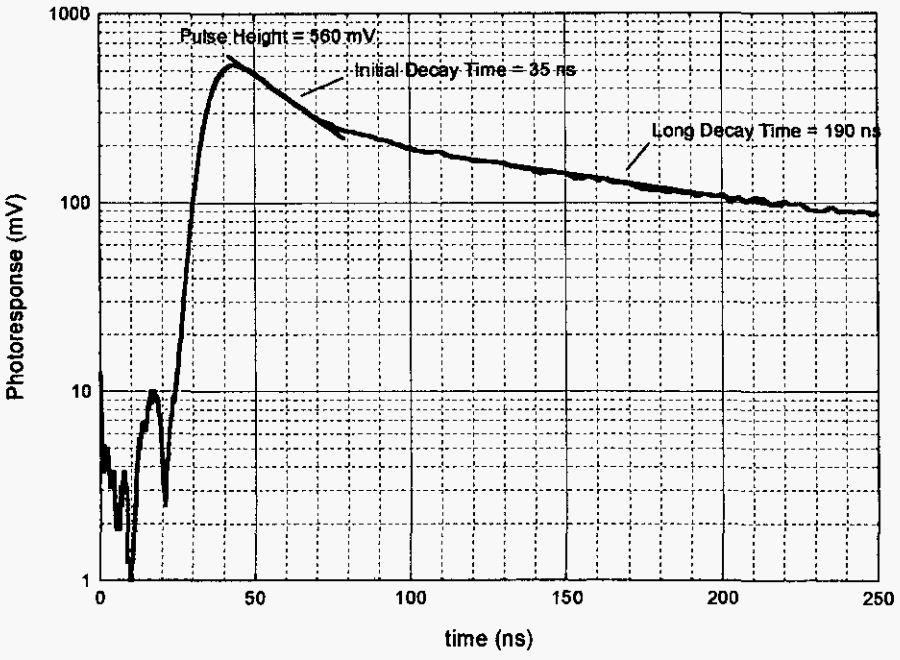

Figure 2. Typical RF Photoreflection response from a GaSb substrate (1064 nm, 100 % intensity)

deflection at the heterointerface, because of the barrier presented by the bandgap discontinuities, significantly reducing the effect of surface or interface recombination. These structures result in surface recombination velocities of the order of $1 - 2 \times 10^3$ cm/s [8]. The TPV device performance of GaSb-capped quaternary samples is discussed by Hitchcock et al. [9].

For a thin doubly-capped structure, the effective decay time of carriers is the sum of contribution from bulk and surface recombination. This is given by the equation,

$$\frac{1}{\tau_{eff}} = \frac{1}{\tau_B} + \frac{S_1 + S_2}{W} \qquad (1)$$

where, τ_{eff} is the effective decay time of the carriers, τ_B is the bulk lifetime, S_1 and S_2 are the front and back SRVs and W is the thickness of the sample. Expressing the bulk lifetime in terms of individual mechanisms and assuming $S_1 = S_2 = S$, the above equation becomes,

$$\frac{1}{\tau_{eff}} = \frac{1}{\tau_{Aug}} + \frac{1}{\tau_{Rad}} + \frac{1}{\tau_{SRH}} + \frac{2S}{W} = CN^2 + BN + \frac{1}{\tau_{SRH}} + \frac{2S}{W} \qquad (2)$$

In the above equation, τ_{Aug}, τ_{Rad}, τ_{SRH} are the Auger, Radiative and Shockley-Reed-Hall lifetimes, C is the Auger coefficient, B is the radiative recombination coefficient and N is the doping concentration.

PC-1D is a computer program which solves the fully coupled nonlinear equations for the quasi-one-dimensional transport of electrons and holes in crystalline semiconductor devices [10]. For the RF photoreflectance simulations, the sample material and structural parameters are first specified. Recombination parameters, including Auger and radiative recombination coefficients and front and back SRVs, are also specified. The sample is excited with a pulse of appropriate wavelength and intensity and the excess sheet conductance of the sample versus time is obtained. The integrated conductivity from the front to the back surface relative to the value at equilibrium is calculated; this value is assumed proportional to the RF photoresponse.

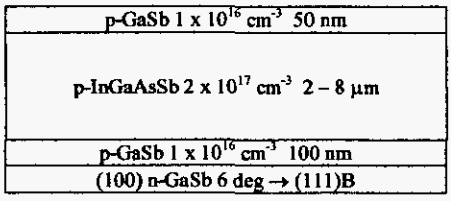

Figure 3. Cross-section of doubly-capped InGaAsSb/GaSb structure

III. PC-1D Simulation Results

The laser pulse used for the PC-1D simulations at 1064 nm and 15 % intensity is shown in Figure 4. The pulse has a full-width half maxima (FWHM) of approximately 14

ns. The 15 % intensity pulse, which has an energy of 0.225 mJ/cm^2, is used for most of the simulations.

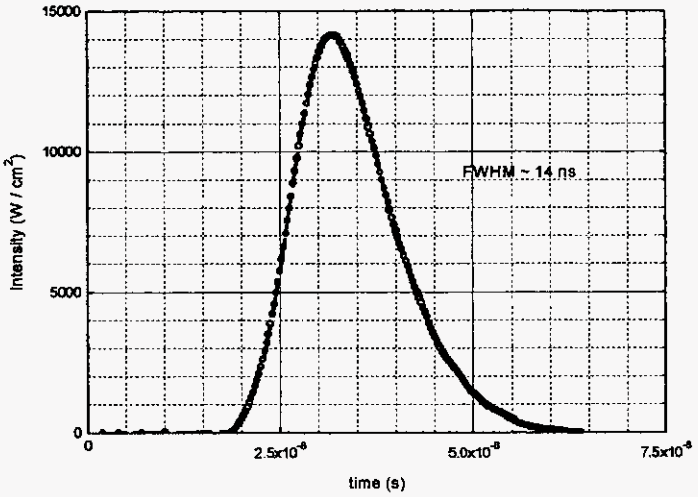

Figure 4. Laser pulse corresponding to 1064 nm wavelength, 15 % intensity. Enclosed area = 0.225 mJ/cm^2

Simulation of GaSb samples

Simulations of thick (500 μm) GaSb substrates are used to study the effect of different recombination parameters on the decay time of the photoconductivity transient. Subsequently, thin GaSb structures (2 μm to 6 μm) are simulated in PC-1D and the obtained decay times are compared with the predicted decay times from equation (2) for different values of SRV.

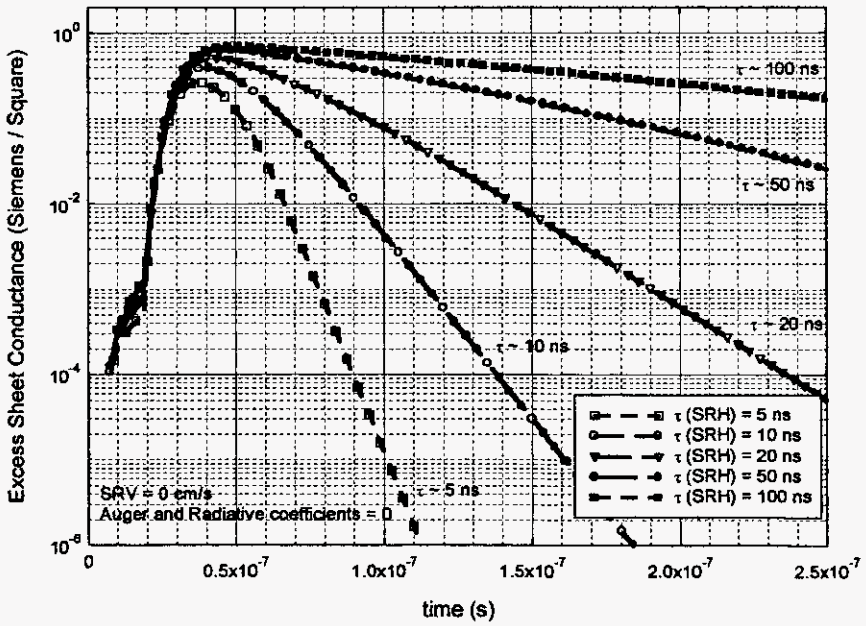

Figure 5. Sheet conductance transients for different values of SRH lifetime, with B=C=0 and SRV = 0 cm/s (1064 nm, 15 % intensity)

Simulations of a 2 x 10^{17} cm^{-3} doped n-GaSb substrate at 1064 nm and 15% intensity are shown in Figure 5. The Auger and radiative recombination coefficients and the surface recombination velocity are set to zero, and the Shockley-Reed-Hall lifetime is varied from 5 ns to 100 ns; in this case the net bulk lifetime is equal to the SRH lifetime. For these transients the low injection level decay time (i.e. long-decay time) of the transient closely matches the SRH lifetime (which is equal to the bulk lifetime) as indicated in Figure 5. This shows that when there is no surface recombination, and there is only one bulk recombination mechanism present, the decay time of the photoconductivity transient obtained using PC-1D is equal to the bulk lifetime, as expected.

The photoconductivity transients at 100 %, 15% and 2 % optical intensities for a 2 x 10^{17} cm^{-3} doped n-GaSb substrate are shown in Figure 6. The following nominal values are used for the recombination parameters: Auger coefficient (C) = 5 x 10^{-30} cm^6/s, radiative recombination coefficient (B) = 7.03 x 10^{-11} cm^3/s, τ_{SRH} = 1000 ns and SRV = 10^7 cm/s. The three transients have low injection level decay (long-decay) times approximately equal to 50 ns and initial decay times of 21 ns, 23 ns and 23 ns, respectively, for the three intensities. This shows that the value of the long decay time is independent of the injection level. Also, for the above values of τ_{SRH}, recombination coefficients and doping, the calculated (from equation (2)) bulk lifetime is 65 ns. The lower value (50 ns) of the long decay time shows that a large value of SRV affects the long decay time of the transient.

The samples used in the experimental results to follow have thin (2 μm to 8 μm) active layers, unlike the thick substrates described above. Simulations of thin n-GaSb samples (with the same bulk recombination parameters as before) were carried out to verify if the decay times obtained with PC-1D agree with the effective decay times

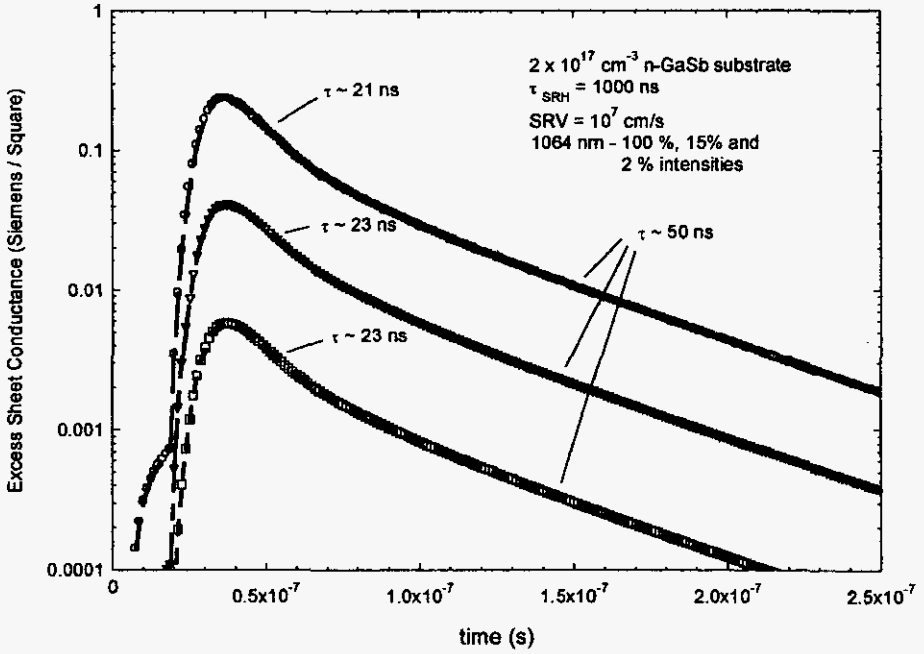

Figure 6. Transients for 2 x 10^{17} cm^{-3} doped n-GaSb substrate (1064 nm; 100 %, 15 % and 2 % intensities)

obtained using equation (2). Table 1 compares the decay times predicted using equation (2) (τ_{Pred}) with the decay times from PC-1D simulation transients (τ_{Sim}) for samples with thicknesses ranging from 2 μm to 6 μm and SRVs from 10^3 to 10^7 cm/s. The calculated decay times are very small (~ 2 ns or lower) for SRVs greater than 10^5 cm/s. A comparison of the two sets of values shows significant agreement between the calculated lifetimes and the simulation results for SRVs in the range 10^3 to 10^4 cm/s. These results confirm the correlation between PC-1D simulation results and the first-order analytical model represented by equation (2).

W (μm)	SRV, S (cm/s)									
	10^7		10^6		10^5		10^4		10^3	
	τ_{Pred} (ns)	τ_{Sim} (ns)	τ_{Pred} (ns)	τ_{Sim} (ns)	τ_{Pred} (ns)	τ_{Sim} (ns)	τ_{Pred} (ns)	τ_{Sim} (ns)	τ_{Pred} (ns)	τ_{Sim} (ns)
2	0.01	< 5	0.1	< 5	0.98	< 5	8.7	10	39.4	36
3	0.015	< 5	0.15	< 5	1.46	< 5	12.2	13	45.4	41
4	0.02	< 5	0.2	< 5	1.94	< 5	15.3	16	49.1	44
6	0.03	< 5	0.3	< 5	2.87	< 5	20.5	22	53.4	45

Table 1. Predicted effective lifetimes using equation (2) (τ_{Pred}) and PC-1D simulated decay times (τ_{Sim}) for n-GaSb doped at 2×10^{17} cm^{-3} ($C = 5 \times 10^{-30}$ cm^6/s, $B = 7.03 \times 10^{-11}$ cm^3/s, $\tau_{SRH} = 1000$ ns)

Simulation of quaternary (InGaAsSb) samples

As mentioned in the introduction, theoretical calculations and experiments give a value in mid-10^{-11} cm^3/s for the radiative recombination coefficient (B) of antimonide materials in the range 0.50 eV to 0.55 eV. However, the reported Auger coefficients have significant variations (10^{-26} to 10^{-29} cm^6/s). A doubly-capped quaternary with bandgap of 0.50 eV was simulated with different parameters to determine the impact of the Auger coefficient on RF photoreflection decay. The simulations use a τ_{SRH} = 1000 ns and radiative recombination coefficient (B) = 6.25×10^{-11} cm^3/s. The Auger coefficient, SRV, sample thickness and doping are varied in the simulations to determine the impact of Auger coefficient.

Table 2 shows the bulk lifetime vs. doping for two values of Auger coefficients differing by an order of magnitude (τ_{SRH} = 1000 ns and $B = 6.25 \times 10^{-11}$ cm^3/s).The bulk lifetime values from this table are used to calculate (using equation (1)) the effective decay time as a function of SRV, sample thickness and doping concentration.

The effective decay times for Auger coefficient (C) = 2.04×10^{-27} cm^6/s are shown in Table 3, while the effective decay times for Auger coefficient (C) = 2.04×10^{-28} cm^6/s are shown in Table 4. Comparing the decay times from Tables 3 and 4, the decay times are ~ 2 ns or less for SRV = 10^5 cm/s, while at 10^4 cm/s, for 2 μm thick samples the difference in decay times for the two Auger coefficients is not significant. However, a

significant difference between the decay times for the two values of Auger coefficients is observed when the SRV is 10^3 cm/s. Therefore, an SRV in the range $\leq 10^3$ cm/s is necessary to differentiate between Auger coefficients using the long decay time of the samples. Also from Tables 3 and 4, at 10^3 cm/s the thicker sample provides increased resolution between the decay times for the two Auger coefficient values.

Auger Coefficient C_n (cm^6/s)	Doping Concentration		
	6×10^{16} cm^{-3}	1.1×10^{17} cm^{-3}	2×10^{17} cm^{-3}
2.04×10^{-27}	82.7 ns	30.7 ns	10.5 ns
2.04×10^{-28}	182 ns	96.7 ns	46.2 ns

Table 2. Bulk Lifetime in InGaAsSb vs. doping concentration for different Auger coefficients (τ_{SRH} = 1000 ns and B = 6.25×10^{-11} cm^3/s)

Doping (cm^{-3})	2 μm			5 μm		
	10^3 (cm/s)	10^4 (cm/s)	10^5 (cm/s)	10^3 (cm/s)	10^4 (cm/s)	10^5 (cm/s)
2.0×10^{17}	9.5 ns	5.1 ns	0.91 ns	10.1 ns	7.4 ns	2.0 ns
1.1×10^{17}	23.5 ns	7.5 ns	0.97 ns	27.3 ns	13.8 ns	2.3 ns
6.0×10^{16}	45.3 ns	8.9 ns	0.99 ns	62.1 ns	19.2 ns	2.4 ns

Table 3. Dependence of effective decay time on SRV and sample thickness for different InGaAsSb doping concentrations ($C_n = 2.04 \times 10^{-27}$ cm^6/s)

Doping (cm^{-3})	2 μm			5 μm		
	10^3 (cm/s)	10^4 (cm/s)	10^5 (cm/s)	10^3 (cm/s)	10^4 (cm/s)	10^5 (cm/s)
2.0×10^{17}	31.6 ns	8.2 ns	0.98 ns	38.9 ns	16.2 ns	2.4 ns
1.1×10^{17}	49.2 ns	9.1 ns	0.99 ns	69.7 ns	19.9 ns	2.4 ns
6.0×10^{16}	64.5 ns	9.5 ns	0.99 ns	105 ns	22.0 ns	2.5 ns

Table 4. Dependence of effective decay time on SRV and sample thickness for different InGaAsSb doping concentrations ($C_n = 2.04 \times 10^{-28}$ cm^6/s)

Figure 7 shows the dependence of the photoconductivity transient on Auger coefficient for a 5 μm thick 0.50 eV quaternary material doped at 2×10^{17} cm^{-3} for three Auger coefficients differing from each other by a half order of magnitude. The rest of the recombination parameters are same as before (τ_{SRH} = 1000 ns, B = 6.25×10^{-11} cm^3/s, front and back SRVs = 10^3 cm/s). The transient decay times from the simulations agree quite well with the calculated effective decay times from equation (1), as shown. Since there is a significant change in the long decay time with change in the Auger coefficient, Figure 7 indicates that the long-decay time of the photoconductivity transient can be used

to estimate the Auger coefficient if the sample doping concentration and thickness are known.

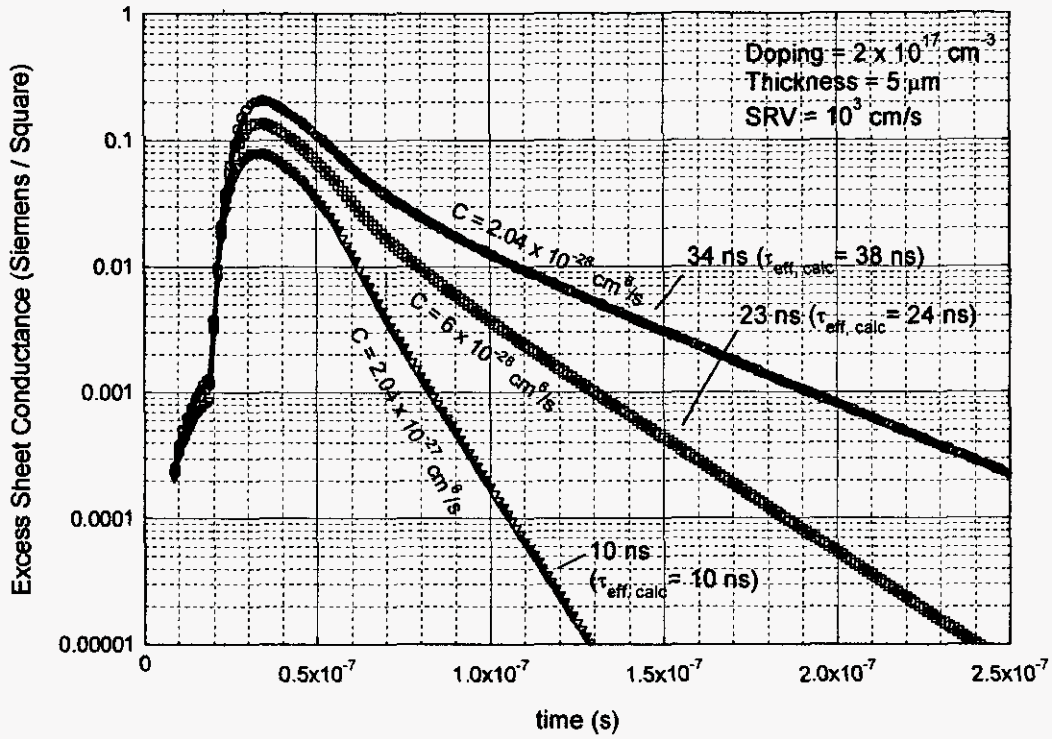

Figure 7. Simulation of photoconductivity transient dependence on Auger coefficient for 0.50 eV InGaAsSb (1064 nm, 15 % intensity).

IV. Experimental Results

RF photoreflection measurements at 1064 nm with 15% intensity were used to characterize samples grown at Lincoln Laboratory (98-870 series). These are variable bandgap, lattice matched 2 μm thick p-InGaAsSb layers with GaSb capping layers at the front and the back, grown on n-GaSb substrates. The active layer is unintentionally doped (~ 1 x 10^{16} cm^{-3}), and the bandgap varies from 0.50 eV to 0.59 eV. All samples have a 0.05 μm thick p-GaSb capping layer at the front and a 0.10 μm thick p-GaSb capping layer at the back. Sample bandgaps and compositions are shown in Table 5.

Sample	Bandgap	Indium Concentration
98-874	0.50 eV	0.235
98-872	0.52 eV	0.200
98-871	0.55 eV	0.169
98-873	0.59 eV	0.122

Table 5: Structure of unintentionally doped p-type InGaAsSb Samples with GaSb Capping Layers (98-870 series). All active layers are 2 μm thick.

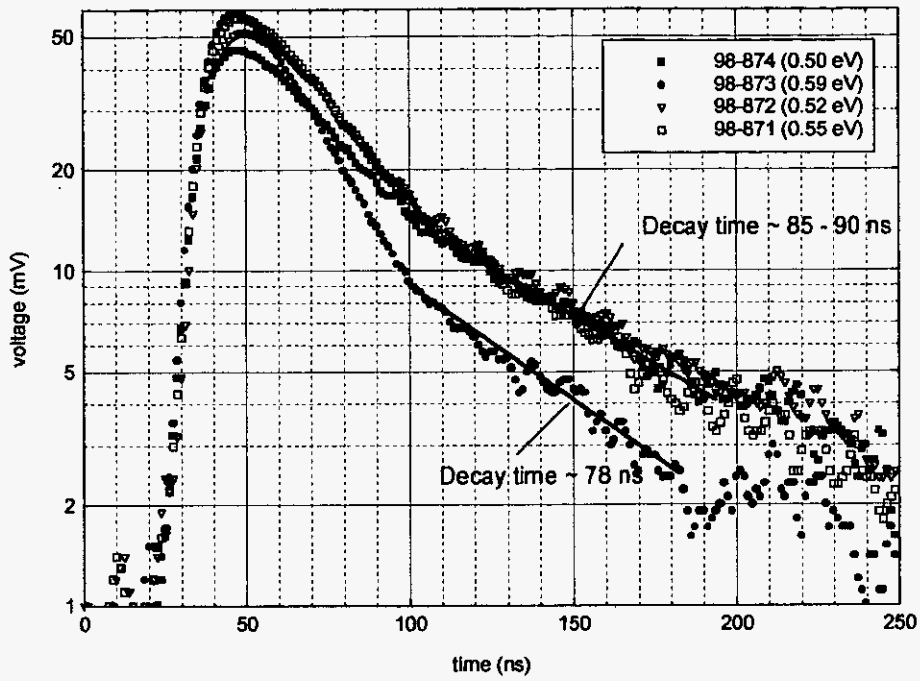

Figure 8. RF photoreflection results for doubly-capped, unintentionally doped lattice matched InGaAsSb samples (1064 nm, 15% intensity). The capping layers are p-doped GaSb.

The results of the RF photoreflection measurements on the above samples are shown in Figure 8. Samples 98-874 (0.50 eV), 98-872 (0.52 eV) and 98-871 (0.55 eV) show a long-decay time of approximately 85 to 90 ns, while 98-873 (0.59 eV) has a slightly shorter long-decay time (78 ns).

At the low doping concentration (~ 10^{16} cm^{-3}) of the 98-870 series samples, the radiative and Auger lifetimes are very large and do not affect the effective decay time. For example, with upper limits of radiative and Auger recombination coefficients (B = 10^{-10} cm^3/s and C = 2 x 10^{-27} cm^6/s), the radiative and Auger lifetimes are both greater than 2 μs at a doping concentration of 10^{16} cm^{-3} and do not significantly affect the long-decay time.

Sample 98-874 is simulated using PC1D with parameters B = 5 x 10^{-11} cm^3/s and C = 10^{-28} cm^6/s and τ_{SRH} = 1 μs; an SRV of 600 cm/s is required to obtain a long-decay time of 85 ns. Sample 98-873, which has the highest bandgap shows a lower long-decay time (78 ns) compared to the other samples. An SRV = 800 cm/s is required to obtain the 78 ns long-decay time with the other recombination parameters the same as above. The higher SRV for this sample may be due to increased surface recombination resulting from a decreased band discontinuity at the InGaAsSb – GaSb interface. Calculating the surface lifetime, W/2S (W = 2 μm), for the two SRVs above gives 166 ns for 600 cm/s and 125 ns for 800 cm/s. This confirms that for these samples the SRV controls the long-decay time.

RF photoreflection measurements (1064 nm, 15% intensity) were also performed on other samples grown at Lincoln Laboratory (98-810 series) with structures shown in Table 6. These are 0.55 eV samples with lattice-matched quaternary active layer thickness varying from 2 μm to 8 μm. These samples also have a 0.05 μm thick p-GaSb

capping layer at the front and a 0.10 μm thick p-GaSb buffer layer at the back. Five samples are doped at 2 x 10^{17} cm^{-3}, and one sample is doped at 1 x 10^{18} cm^{-3}.

Sample	Bandgap	Active Layer Thickness	Active Layer Doping
98-813	0.55 eV	2 μm	2 x 10^{17} cm^{-3}
98-814	0.55 eV	3 μm	2 x 10^{17} cm^{-3}
98-815	0.55 eV	5 μm	2 x 10^{17} cm^{-3}
98-816	0.55 eV	8 μm	2 x 10^{17} cm^{-3}
98-817	0.55 eV	3 μm	1 x 10^{18} cm^{-3}

Table 6: Structure of p-type InGaAsSb Samples with GaSb capping layers (98-810 series)

Samples 98-813 to 98-816 show long-decay times varying from 38 ns to 57 ns as shown in Figure 9. The 1 x 10^{18} cm^{-3} doped sample (98-817) has no long-decay time. Sample 98-814 was simulated using PC-1D, with Auger and radiative recombination coefficients, SRH lifetime and SRV modified to obtain a long-decay time of 42 ns; the following material parameters were obtained: B= 5 x 10^{-11} cm^3/s, C= 1 x 10^{-28} cm^6/s, τ_{SRH} = 1 μs and SRV (front and back) = 600 cm/s. The 1 x 10^{18} cm^{-3} doped sample in the series (98-817) did not have a long-decay time, which could be attributed to the low net bulk lifetime (6.7 ns) obtained with the parameters above (B= 5 x 10^{-11} cm^3/s and C= 1 x 10^{-28} cm^6/s).

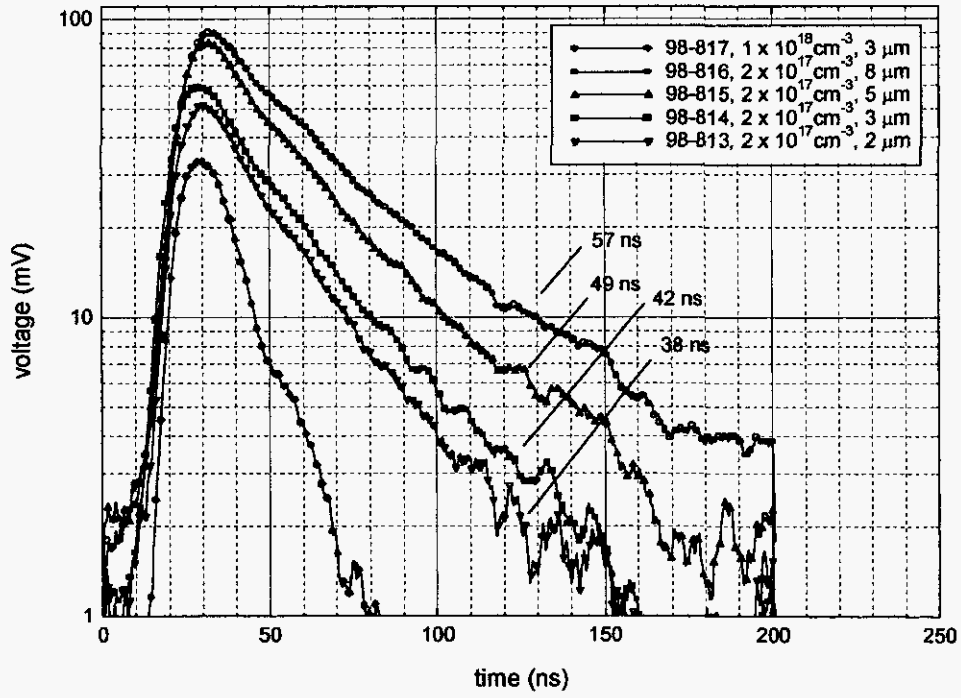

Figure 9. RF photoreflection results for doubly-capped, lattice matched InGaAsSb samples (1064 nm, 15% intensity). The capping layers are p-doped GaSb.

Sample	Bandgap	Active Layer Thickness	Active Layer Doping
Itv-1028	0.55 eV	1 μm	1×10^{18} cm^{-3}
Itv-1027	0.55 eV	2 μm	1×10^{18} cm^{-3}
Itv-1030	0.55 eV	5 μm	1×10^{18} cm^{-3}
Itv-1052	0.55 eV	3 μm	1×10^{17} cm^{-3}

Table 7: Structure of p-type InGaAsSb Samples with GaSb capping layers (itv-1000 series)

The parameters obtained above for sample 98-814 (B = 5×10^{-11} cm^3/s, C= 1×10^{-28} cm^6/s, τ_{SRH} = 1 μs and SRV (front and back) = 600 cm/s) were used to simulate the photoresponse of the three other samples in the series: 98-813 (2 μm), 98-815 (5 μm) and 98-816 (8 μm). The simulations give long-decay times of 40 ns, 48 ns and 54 ns respectively for the three samples. These values agree reasonably well with the experimental decay times obtained for the above samples (38 ns, 49 ns and 57 ns, respectively), indicating that the parameters obtained for 98-814 are applicable to all the samples in the series.

The RF photoreflection results at 1064 nm (100% intensity) for itv-1000 series samples grown at Sarnoff Corporation are shown in Figure 10. The results at 100 % intensity are used because the photoresponse at 15 % intensity had smaller amplitudes compared to the earlier two series of samples and the long decay times could not be reliably measured. The structure of the four samples is shown in Table 7. The Sarnoff itv-1000 series consists of 0.55 eV quaternary samples with 100 nm GaSb front and back

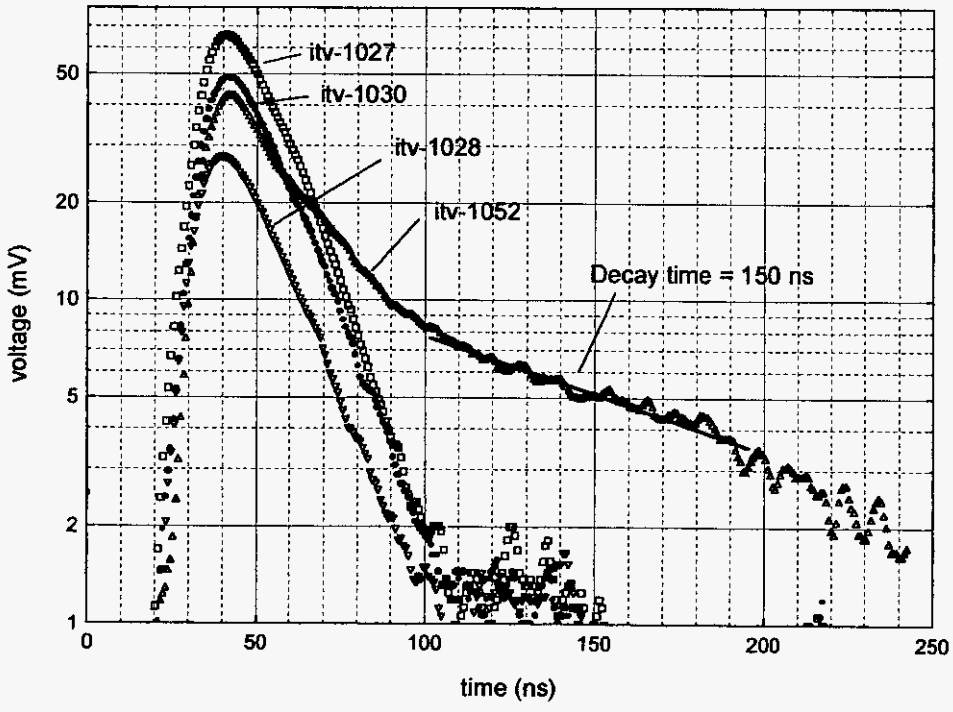

Figure 10. RF photoreflection results for doubly-capped, lattice matched InGaAsSb samples (1064 nm, 100% intensity). Capping layer is p-doped GaSb.

capping layers. Three samples are doped at 1 x 10^{18} cm^{-3} and one sample at 1 x 10^{17} cm^{-3}. The 10^{17} cm^{-3} doped sample has a long-decay time of ~ 150 ns and the three 10^{18} cm^{-3} doped samples have long-decay times that are too low to be measured. This latter behavior, similar to that of the sample 98-817 in the Lincoln Laboratory 98-810 series, can again be attributed to the low bulk lifetimes resulting from the high doping concentration.

PC-1D was used to simulate the decay time (150 ns) of sample itv-1052. However, with the simulations a long decay time as large as 150 ns could not be obtained using material parameters consistent with the previously described values (SRV greater than 400 cm/s, B greater than 10^{-11} cm^3/s and C greater than 2 x 10^{-29} cm^6/s). A decay time of ~ 130 ns obtained with the following parameters: B= 1 x 10^{-11} cm^3/s, C= 2 x 10^{-29} cm^6/s, τ_{SRH} = 10 μs and SRV = 400 cm/s is considered to be the best fit with reasonable material parameters. The longer decay time observed in this sample may be due to the effect of trapping or photon recycling.

The above simulations and conclusions assume accurate characterization of the doping concentrations of these low band gap samples; the recombination parameters (mainly the Auger coefficient) were modified to obtain a decay time compatible with the experimental results. However, higher values of the Auger coefficient combined with a lower active-layer doping concentration can also result in decay times compatible with the experimental results. Assuming an Auger coefficient an order of magnitude larger (2 x 10^{-27} cm^6/s), the doping concentration of the samples was decreased to obtain a decay time equal to the experimental results. For sample 98-814 (long decay time = 42 ns), assuming an Auger coefficient of 2 x 10^{-27} cm^6/s, a doping concentration of approximately 7 x 10^{16} cm^{-3} is required to obtain the 42 ns long-decay time compared to the characterized value of 2 x 10^{17} cm^{-3}. Similar results were obtained for other samples in the 98-810 series. Since the 98-870 series samples are lightly doped, the effect of changing the doping concentration cannot be used to delineate between Auger recombination parameters, since the Auger lifetime is large. In all the simulations, the effect of photon recycling (carrier-generation due to absorption of photons emitted during radiative recombination) is neglected. Photon recycling, if present, would increase the effective radiative lifetime of the sample [11].

V. Summary and Conclusions

PC-1D simulations and lifetime measurements using RF photoreflection have been carried out to obtain improved values of recombination parameters for doubly-capped lattice matched InGaAsSb samples in the 0.50 eV to 0.59 eV range. PC-1D simulations show that the long-decay times of the photoconductivity transients, after taking into account the effect of SRV, can be used to obtain the effective lifetime of minority carriers and, with well characterized samples of variable doping concentration and thickness, fundamental recombination parameters.

RF photoreflection measurements and PC-1D simulations with a 0.55 eV, 3 μm thick, 2 x 10^{17} cm^{-3} doped sample (98-814) show a radiative recombination coefficient (B) = 5 x 10^{-11} cm^3/s and Auger coefficient (C) = 1 x 10^{-28} cm^6/s. Simulations with the same parameters give long-decay times of 40 ns, 48 ns and 54 ns respectively for the three other samples in the series: 98-813 (2 μm), 98-815 (5 μm) and 98-816 (8 μm).

These values agree well with observed experimental results. Sample 98-874 (0.50 eV, 2 um, 1 x 10^{16} cm^{-3} doped) shows an SRV of 600 cm/s, slightly lower than previous estimates for InGaAsSb/GaSb materials [8]. The lower decay time of the higher bandgap (0.59 eV) GaSb capped quaternary sample is attributed to slightly increased surface recombination resulting from a decreased band discontinuity at the InGaAsSb – GaSb interface; an SRV = 800 cm/s was obtained for this sample.

The low decay times observed for the 1 x 10^{18} cm^{-3} doped samples (98-817, itv-1027, itv-1028 and itv-1030) are attributed to increased Auger recombination. With B= 5 x 10^{-11} cm^3/s and C = 1 x 10^{-28} cm^6/s, the 1 x 10^{18} cm^{-3} doped sample has a calculated bulk decay time of ~ 6.7 ns. For sample itv-1052 (0.55 eV, 1 x 10^{17} cm^{-3}, 3 μm thick) a long-decay time of ~ 150 ns was observed with the RF photoreflection measurements. A decay time of ~ 130 ns obtained in PC-1D with the following parameters: B= 1 x 10^{-11} cm^3/s, C= 2 x 10^{-29} cm^6/s, τ_{SRH} = 10 μs and SRV = 400 cm/s is considered the best fit. The longer decay time of this sample may be due to the effect of trapping of minority carriers or photon recycling.

Accurate doping concentrations in low band gap lattice-matched quaternary layers on doped GaSb substrates are necessary for accurate experimentally-based values of recombination parameters. Dependence of Auger and radiative recombination lifetimes on the doping concentration can be plotted using the equations $\tau_{Rad} = 1/BN$ and $\tau_{Auger} = 1/CN^2$. With the experimentally-based recombination coefficients (B= 5 x 10^{-11} cm^3/s and C= 2 x 10^{-28} cm^6/s) Auger recombination becomes the dominant bulk recombination mechanism at doping levels above ~ 4 x 10^{17} cm^{-3}; at lower doping levels radiative recombination is dominant. If the Auger coefficients are higher, Auger recombination becomes the dominant bulk recombination at lower doping concentrations. This difference can be critical in design of antimonide-based minority carrier devices, particularly TPV cells and photodetectors.

Acknowledgments

The authors would like to thank Dr. Sudesh Saroop (formerly at RPI and now at IBM) for development of the RF photoreflection setup and previous characterization, Dr. Greg Charache (formerly at Lockheed Martin) for many technical discussions and Mr. Greg Nichols of Lockheed Martin for program coordination and guidance.

1. P. S. Dutta, H. L. Bhat, and V. Kumar, "The physics and technology of gallium antimonide: An emerging optoelectronic material", Journal of Applied Physics, Volume 81, Number 9, pp. 5821 – 5870 (May 1997).
2. R. U. Martinelli, D. Z. Garbuzov, H. Lee, N. Morris, T. Odubanjo, G. C. Taylor, and J. C. Connolly, "Minority-carrier transport in InGaAsSb thermophotovoltaic diodes", AIP Conference Proceedings, 401, 389 (1997).
3. S. Saroop, J. M. Borrego, R. J. Gutmann, G. W. Charache, and C. A. Wang, 40th Electronic Materials Conference, Charlottesville, VA (1998).
4. G. W. Charache, P. F. Baldasaro, L. R. Danielson, D. M. DePoy, M. J. Freeman, C. A. Wang, H. K. Choi, D. Z. Garbuzov, R. U. Martinelli, V. Khalfin, S. Saroop, J. M. Borrego, and R. J. Gutmann, "InGaAsSb thermophotovoltaic diode: Physics

evaluation", Journal of Applied Physics, Volume 85, Number 4, pp. 2247 – 2252 (Feb 1999).
5. M. E. Flatté C. H. Grein, H. Ehrenreich, R. H. Miles, and H. Cruz, "Theoretical performance limits of 2.1-4.1 μm InAs/InGaSb, HgCdTe, and InGaAsSb lasers", Journal of Applied Physics, Volume 78, Number 7, pp. 4552-4559 (October 1995).
6. C. H. Grein, P. M. Young, M. E. Flatté and H. Ehrenreich, "Long Wavelength InAs/InGaSb Infrared Detectors: Optimization of Carrier Lifetimes" Journal of Applied Physics, Volume 78, Number 12, pp. 7143-7152 (December 1995).
7. R. K. Ahrenkiel, "Contactless measurement of recombination lifetime in photovoltaic materials", Proceedings of the 1997 IEEE 26th Photovoltaic Specialists Conference, Anaheim, CA, USA, pp. 119-122 (1997).
8. S. Saroop, J. M. Borrego, R. J. Gutmann, G. W. Charache, and C. A. Wang, "Recombination processes in Doubly-capped antimonide-based quaternary thin films", Journal of Applied Physics, Volume 86, Number 3, pp. 1527 – 1534 (August 1999).
9. C. W. Hitchcock, R. J. Gutmann, H. Ehsani, I.B. Bhat, C.A. Wang, M.J. Freeman, and G.W. Charache, "Ternary and quaternary antimonide devices for thermophotovoltaic applications", Journal of Crystal Growth, Volume 195, Number 1-4, pp. 363 – 372 (December 1998).
10. "PC 1D Version 5", 26th IEEE Photovoltaic Specialists Conference, Anaheim (Sep-Oct 1996).
11. J. M. Borrego, S. Saroop, R. J. Gutmann, G. W. Charache, T. Donovan, P. F. Baldasaro, and C. A. Wang, "Photon recycling and recombination processes in 0.53 eV p-type InGaAsSb", Journal of Applied Physics, Volume 89, Number 7, pp. 3753 – 3759 (April 2001).